Submitted to *Biological Cybernetics*, January 2004.

OPTIMIZATION BASED TRAJECTORY PLANNING OF HUMAN UPPER BODY

by

Karim Abdel-Malek[1], Jingzhou Yang[1]*, Zan Mi[1], and Kyle Nebel[2]

[1]Virtual Soldier Research Program
Center for Computer-Aided Design
The University of Iowa
116 Engineering Research Facility
Iowa City, IA 52242-1000
Tel: (319) 353-2249
Fax: (319) 384-0542
www.digital-humans.org

[2]U.S. Army TACOM/RDECOM
AMSRD-TAR-NAC/157
6501 East 11 Mile Rd.
Warren, MI 48397-5000
Ph (586)574-8809
Fax (586)574-6280

E-mail: **jyang@engineering.uiowa.edu**

Original Submission: January 2004

* Author to whom all correspondence should be addressed

Report Documentation Page

Form Approved
OMB No. 0704-0188

1. REPORT DATE	2. REPORT TYPE	3. DATES COVERED
01 JAN 2004	**Technical Report**	**01-01-2003 to 01-01-2004**

4. TITLE AND SUBTITLE
OPTIMIZATION BASED TRAJECTORY PLANNING OF HUMAN UPPER BODY

5a. CONTRACT NUMBER
DAAE07-03-D-L003

5b. GRANT NUMBER

5c. PROGRAM ELEMENT NUMBER

6. AUTHOR(S)
Kyle Nebel; Jing Yang; Karim Abdel-Malek

5d. PROJECT NUMBER

5e. TASK NUMBER

5f. WORK UNIT NUMBER

7. PERFORMING ORGANIZATION NAME(S) AND ADDRESS(ES)
Virtual Soldier Research Program,The University Of Iowa,116 Engineering Research Facility,Iowa City,IA,52242-1000

8. PERFORMING ORGANIZATION REPORT NUMBER
#

9. SPONSORING/MONITORING AGENCY NAME(S) AND ADDRESS(ES)
U.S. Army TARDEC, 6501 E.11 Mile Rd, Warren, MI, 48397-5000

10. SPONSOR/MONITOR'S ACRONYM(S)

11. SPONSOR/MONITOR'S REPORT NUMBER(S)
#13984

12. DISTRIBUTION/AVAILABILITY STATEMENT
Approved for public release; distribution unlimited

13. SUPPLEMENTARY NOTES

14. ABSTRACT

Many tasks require the arm to move from its initial position to a specified target position without any constraints or via a point for a curved path in case of obstacle avoidance. In this paper we presented a formulation to plan the trajectory of human upper body. Having obtained the desired path in Cartesian space using the minimum jerk theory and represented each joint motion by a B-spline curve with unknown parameters (i.e., control points), an optimization approach instead of inverse kinematics is used to predict control points of each joint?s profile (a spline curve). It forms an optimization problem and the cost function includes four parts: (1). The discomfort function that evaluates displacement of each joint away from its neutral position; (2). The consistency function, which is the joint rate change (first derivative) and predicted overall trend from the initial point to the end point; (3). The non smoothness function of the trajectory, which is the second derivative of the joint trajectory; (4). The non continuity function, which is the amplitudes of joint angle rates at the start and end points In order to emphasize smooth starting and ending conditions. This paper presents a high redundancy the upper body modeling with 15 degrees of freedom and optimization approach to predict the trajectory of human upper body. It can be expandable to apply the formulation to other parts of the human body. Illustrative examples were presented and an interface was set up to visualize the results.

15. SUBJECT TERMS

Key Words: Planning trajectory, biomechanics, minimum jerk, B-slines, joint space.

16. SECURITY CLASSIFICATION OF:			17. LIMITATION OF ABSTRACT	18. NUMBER OF PAGES	19a. NAME OF RESPONSIBLE PERSON
a. REPORT **unclassified**	b. ABSTRACT **unclassified**	c. THIS PAGE **unclassified**	**Same as Report (SAR)**	**32**	

Standard Form 298 (Rev. 8-98)
Prescribed by ANSI Std Z39-18

Abstract

Many tasks require the arm to move from its initial position to a specified target position without any constraints or via a point for a curved path in case of obstacle avoidance. In this paper we presented a formulation to plan the trajectory of human upper body. Having obtained the desired path in Cartesian space using the minimum jerk theory and represented each joint motion by a B-spline curve with unknown parameters (i.e., control points), an optimization approach instead of inverse kinematics is used to predict control points of each joint's profile (a spline curve). It forms an optimization problem and the cost function includes four parts: (1). The *discomfort function* that evaluates displacement of each joint away from its neutral position; (2). The *consistency function*, which is the joint rate change (first derivative) and predicted overall trend from the initial point to the end point; (3). The *non smoothness function* of the trajectory, which is the second derivative of the joint trajectory; (4). The *non continuity function*, which is the amplitudes of joint angle rates at the start and end points In order to emphasize smooth starting and ending conditions. This paper presents a high redundancy the upper body modeling with 15 degrees of freedom and optimization approach to predict the trajectory of human upper body. It can be expandable to apply the formulation to other parts of the human body. Illustrative examples were presented and an interface was set up to visualize the results.

Key Words: Planning trajectory, biomechanics, minimum jerk, B-slines, joint space.

Introduction

In industrial applications the movement of the robot manipulators are planned in two ways: The first approach requires the user to explicitly specify a set of constraints (e.g., continuity and smoothness) on position, velocity, and acceleration of the manipulator's generalized coordinates at selected locations (called knot points or interpolation points) along the trajectory. The trajectory planner then selects a parameterized trajectory from a class of functions (usually the class of polynomial functions of degree n or less, for some n), in the time interval $\left[t_0 \quad t_f\right]$ that "interpolates" and satisfies the constraints at the interpolation points. In the second approach, the user explicitly specifies the path that the manipulator must traverse by an analytical function, such as a straight-line path in Cartesian coordinates, and the trajectory planner determines a desired trajectory either in joint coordinates or Cartesian coordinates that approximates the desired path.

Prediction of human motions and postures is particularly difficult because of two main reasons: (i) the large number of degrees of freedom that is required to model realistic motion and (ii) the inverse kinematic solution (i.e., predicting a posture) is not as straightforward as in the case of robots, because while many solutions are mathematically admissible, they do not make sense and are unrealistic! This has been a long standing problem in human modeling, simulation, and ergonomics. Indeed, traditional algebraic and geometric IK methods are difficult to implement and yield an infinite number of solutions, one of which must be selected. Some numerical IK methods have been used to

solve low degree-of-freedom human models. For human models, a realistic solution must be determined, one that resembles the actual motion.

By using a quaternion to represent rotations and translations, Taylor (1979) proposed an approach, called bounded deviation joint path. This approach requires a motion planning phase that selects enough knot points so that the manipulator can be controlled by linear interpolation of joint values.

Significant research has also been done on collision free motion planning. For example, in the early 1980s, Lozano-Perez (1984) introduced the concept of a robot's configuration space, in which the robot is represented as a point–called a configuration– in a parameter space encoding the robot's DOFs–the configuration space. Path planning for a dimensioned robot is thus "reduced" to the problem of planning a path for a point in a space that has as many dimensions as the robot has DOFs. Two popular approaches were introduced in the 1980s: approximate cell decomposition, where the free space is represented by a collection of simple cells (Brooks and Lozano-Perez, 1983), and potential field (Khatib, 1986). Potential fields are used in path planning to create regions with numeric values that give an indication of a measure of safety of that region. But none of these approaches extends well to robots with more than 4 or 5 DOFs, either the number of cells becomes too large or the potential field has local minima.

Because the common invariant features of these movements were only evident in the extracorporal coordinates of the hand, there is a strong indication that planning takes

place in terms of hand trajectories rather than joint rotations. Flash and Hogan (1985) presented a mathematical model which was shown to predict both the qualitative features and the quantitative details observed experimentally in planar, multi-joint arm movements. The objective function is the square of the magnitude of jerk (rate of change of acceleration) of the hand integrated over the entire movement. This is equivalent to assuming that a major goal of motor coordination is the production of the smoothest possible movement of the hand.

The observation that unconstrained, unperturbed arm movements are coordinated in terms of hand motion shows that motor control is organized in a hierarchy of increasing levels of abstraction (Hogan *et al*., 1987). These arm motions are organized as though a disembodied hand could be moved in space; the details of how this is achieved must then be supplied by a different level in the hierarchy.

Other models have also been proposed and studied. The comparison of Nelson (1983) showed the remarkable similarity of movements predicted by the linear-spring model and minimum-jerk model. Uno *et al*. (1989) proposed a mathematical model, which is formulated by defining an objective function, square of the rate of change of torque integrated over the entire movement.

Kawato *et al.* (1988) studied the problems of coordinates transformation from the desired trajectory to the body coordinates and motor command generation. They proposed an

iterative learning control as an algorithm for simultaneously solving these two problems. This approach appears to be very attractive, but it lacks capability of generalization.

Bobrow (1988) presented a path planning technique, which makes use of approximations of an initial feasible trajectory in conjunction with an iterative, nonlinear parameter optimization algorithm to produce time-optimal motions for a manipulator with 3 DOF's in a workspace containing obstacles. The Cartesian path of the manipulator was represented with B-spline polynomials, and the shape of this path was varied in a manner that minimized the traversal time. Obstacle avoidance constraints were included in the problem through the use of distance functions. His method did not prevent the arm from colliding with the obstacle at points other than the tip.

A randomized planner was introduced (Barraquand and Latombe, 1991), which was able to solve complex path-planning problems for many-DOF robots by alternating "down motions" to track the negated gradient of a potential field and "random motions" to escape local minima. Later, a probabilistic roadmap (PRM) planner (Kavraki *et al.*, 1996) was developed. By sampling the configuration space by "local" paths (typically straight paths), a PRM can be created. Samples and local paths are checked for collision using a fast collision checker, which avoids the prohibitive computation of an explicit representation of the free space.

Yun and Xi (1996) used genetic algorithms for optimum motion planning in joint space for robot, where some inter-knots were selected and their parameters and the traveling

time of each trajectory segment were coded and optimized. Similarly, Constantinescu and Croft (2000) put up with a smooth and time-optimal trajectory planning which minimizes time under path constraints, torque limits and torque rate limits. The variables of the optimization are the end-effector pseudo-velocities at the preselected knot-points along the path and the slopes of the trajectory in the $s-\dot{s}$ phase plane at the path end-points, where s is the path parameter, e.g., the arc length. The path itself is pre-imposed as a constraint.

Quinlan and Khatib (1993) put up with an elastic band concept. The free space around the path was represented as a series of hyperspheres, called bubbles. A bubble represents a region of configuration space that is free of collision. Covering the path with those bubbles, a channel of free space was formed through which the robot's trajectory could be executed. Later, Khatib *et al*. (1999) used elastic strip method for the collision-free path modification behaviors of the robots. An elastic strip represents the workspace volume swept by a robot along a preplanned trajectory. This representation was incrementally modified by external repulsive forces originating from obstacles to maintain a collision-free path.

Barring particular overriding circumstances, natural movements–and, more markedly, hand movements–tend to be smooth and graceful. One can then postulate that this characteristic feature corresponds to a design principle, or, in other words, that maximum smoothness is a criterion to which the motor system abides in the planning of end-point movements. Point-to-point movements performed under a wide variety of conditions

using a wide variety of limb segments exhibit the same velocity pattern (Flash and Hogan, 1985; Hogan and Flash, 1987): a smooth, bell-shaped time course, typically symmetrical (or nearly so) about the mid-point of the movement, starting from zero, growing to a single peak and declining again to zero. Many researchers have also reported that the velocity profiles of rapid-aimed movements have a global asymmetric bell-shape, which is invariant over a wide range of movement sizes and speeds, and asymmetry increased with higher accuracy demands (Plamondon, 1995, Part I, Part II; Plamondon, 1998).

Wolpert et al. (1995) have studied the effects of artificial visual feedback on planar two-joint arm movements to distinguish between the two main groups of human trajectory planning models–those specified in kinematic coordinates and those specified in dynamic coordinates. Their results suggested that trajectories are planned in visually based kinematic coordinates, and the desired trajectory is straight in visual space, which is incompatible with purely dynamic-base models such as the minimum torque change model.

Considerable research has been done to obtain optimal robot path. Saramago *et al*. (1998; 2000; 2002) have studied robot path with considering dynamic system, with payload constraints, and in the presence of moving obstacles. Pugazhenthi, *et al.* (2002) studied the optimal trajectory planning for Stewart platform based machine tools. Li and Ceglarek (2002) presented another application of optimal trajectory planning for material

handeling of compliant sheet metal parts with considering part permanent deformation, trajectory smoothness, and static obstacle avoidance.

Alexander (1997) proposed the hypothesis that trajectories are chosen to minimize metallic energy costs. Ohta *et al*. (2003) presented a criterion minimizing the hand contact force change and muscle force change over the time of movement.

Existing approaches are applied in trajectory planning of manipulators which normally have only 2 to 3 DOFs and up to 6 at most. On the other hand, for the realistic motion generation, human models normally have more than 10 DOFs. Moreover, the criteria used for motion planning will be quite different. For example, time optimum is always selected for the manipulator trajectory planning in application. But for human motion, this is not always important; instead, human tends to adopt the motion with least discomfort, effort and most smoothness. This leads to a different research area where different strategies will be used in human motion planning.

This paper presents a methodology to predict and simulate the path generated by humans in a natural motion of the torso and upper extremity. While this work has been limited to a 15 degree of freedom of the upper body, the theory presented herein is expandable to any part of the body that can be represented as segmental links of a kinematic chain. The work is based on a mathematical postulate that allows for the prediction of naturalistic human motion using an optimization-based approach.

Human Modeling

To establish a systematic method for biomechanically modeling human anatomy, researchers have implemented conventions for representing segmental links and joints. Human anatomy can be represented as a sequence of rigid bodies (*links*) connected by *joints*. Of course, this serial linkage could be an arm, a leg, a finger, a wrist, or any other functional mechanism. Joints in the human body vary in shape, function, and form. The complexity offered by each joint must also be modeled, to the extent possible, to enable a correct simulation of the motion. The degree by which a model replicates the actual physical model is called the level of *fidelity*.

Perhaps the most important element of a joint is its function, which may vary according to the joint's location and physiology. The physiology becomes important when we discuss the loading conditions of a joint. In terms of kinematics, we shall address the function in terms of the number of degrees of freedom associated with its overall movement. Muscle action, ligament, and tendon at a joint are also important and contribute to the function.

For example, consider the elbow joint, which is considered a hinge or one degree-of-freedom (DOF) rotational joint (e.g., the hinge of a door) because it allows for flexibility and extension in the sagittal plane (Figure 1) as the radius and ulna rotate about the humerus. We shall represent this joint by a cylinder that rotates about one axis and has no other motions (i.e., 1 DOF). Therefore, we can now say that the elbow is

characterized by one DOF and is represented as a cylindrical rotational joint also shown in Figure 1.

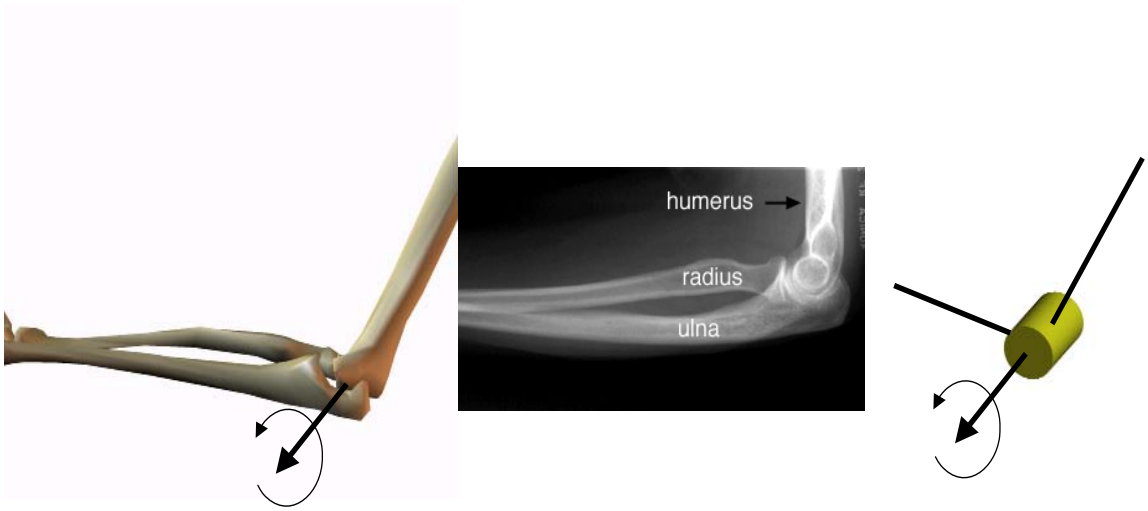

Figure 1 One DOF elbow

On the other hand, consider the shoulder complex (Figure 2). The glenohumeral joint (shoulder joint) is a multi-axial (ball and socket) synovial joint between the head of the humerus (5) and the glenoid cavity (6). There is a 4 to 1 incongruency between the large round head of the humerus and the shallow glenoid cavity. A ring of fibrocartilage attaches to the margin of the glenoid cavity forming the glenoid labrum. This serves to form a slightly deeper glenoid fossa for articulation with the head of the humerus.

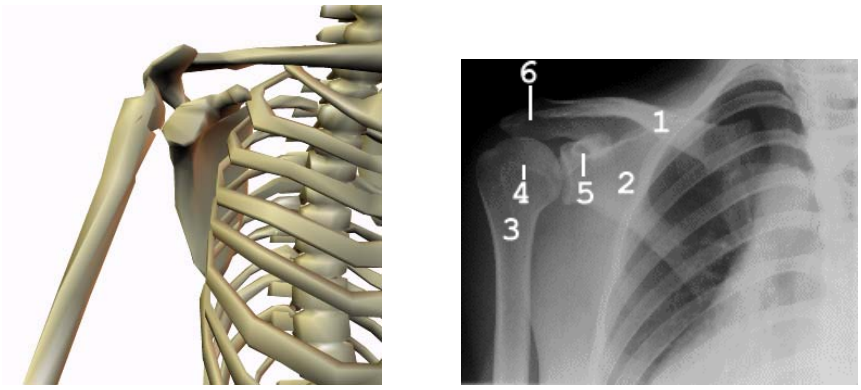

Figure 2 The shoulder joint (1. Clavicle. 2. Body of scapula. 3. Surgical neck of humerus. 4. Anatomical neck of humerus. 5. Coracoid process. 6. Acromion)

We take into consideration the final gross movement of the joint (Abdel-Malek, *et al.* 2001; Yang *et al.*, 2003), as abduction/adduction (about the anteroposterior axis of the shoulder joint), flexion/extension and transverse flexion/extension (about the mediolateral axis of the shoulder joint). Note that these motions provide for three rotational degrees of freedom having their axis intersecting at one point. This gives rise to the effect of a spherical joint typically associated with the shoulder joint (Figure 3). In addition, the upward/downward rotation of the scapula gives rise to two substantial translational degrees of freedom and total 5 DOFs in the shoulder complex. This model allows for consideration of the coupling between some of the joints as is the case in the shoulder where muscles extend over more than one segment. When muscles are used to lift the arm in a rotational motion, unwittingly, a translational motion of the shoulder occurs.

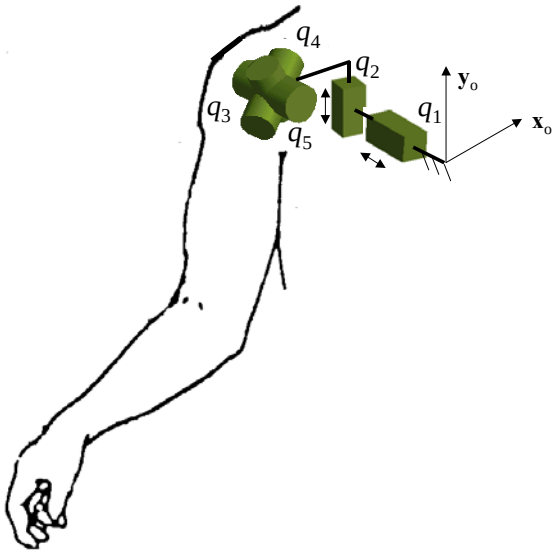

Figure 3 Modeling of the shoulder complex as three revolute and two prismatic DOFs

The normal anatomy of the spine is usually described by dividing up the spine into 3 major sections: the cervical, the thoracic, and the lumbar spine (Figure 4). Below the lumbar spine is a bone called the sacrum, which is part of the pelvis. Each section is made up of individual bones called vertebrae. There are 7 cervical vertebrae, 12 thoracic vertebrae, and 5 lumbar vertebrae.

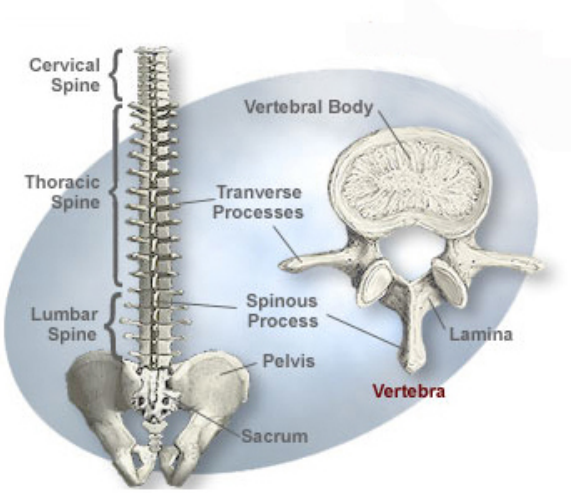

Figure 4 Anatomy of the spine

The movements permitted in the vertebral column are: flexion, extension, lateral movement, circumduction, and rotation. Flexion, or movement forward, is the most extensive of all the movements of the vertebral column, and is freest in the lumbar region. Extension, or movement backward, is limited by the anterior longitudinal ligament. It is freest in the cervical region. The extent of lateral movement is limited by the resistance offered by the surrounding ligaments. This movement may take place in any part of the column, but is freest in the cervical and lumbar regions. Circumduction is very limited, and is merely a succession of the preceding movements. Rotation is produced by the twisting of the intervertebral fibrocartilages. This, although only slight between any two vertebrae, allows of a considerable extent of movement when it takes place in the whole length of the column, the front of the upper part of the column being turned to one or other side. This movement occurs to a slight extent in the cervical region, is freer in the upper part of the thoracic region, and absent in the lumbar region. Since the reach movement of hand is not related to the position of the head, the cervical

part of the spine (neck) is not included in our spine model. The other parts, thoracic region and lumbar region are modeled as 6 DOF rotations as shown in Figures 6.

The wrist is a collection of many joints and bones with one main purpose, to allow human to use the hands. The wrist has to be extremely mobile. At the same time, it has to provide the strength for gripping. The wrist (Figure 5) comprises eight separate small bones called the carpal bones. These bones connect the two bones of the forearm, the radius and the ulna, to the bones of the hand and fingers. The movements permitted in the wrist joint are flexion, extension, abduction and adduction. The wrist-joint is a condyloid articulation. The parts forming it are the lower end of the radius and under surface of the articular disk above; and the navicular, lunate, and triangular bones below. The articular surface of the radius and the under surface of the articular disk form together a transversely elliptical concave surface, the receiving cavity. The superior articular surfaces of the navicular, lunate, and triangular form a smooth convex surface, the condyle, which is received into the concavity. The wrist is modeled as a joint with 3 DOFs as shown in Figures 6.

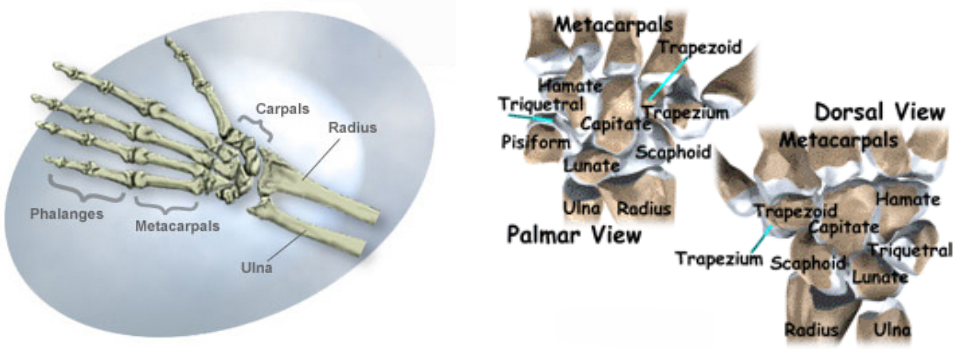

Figure 5 Anatomy of the wrist

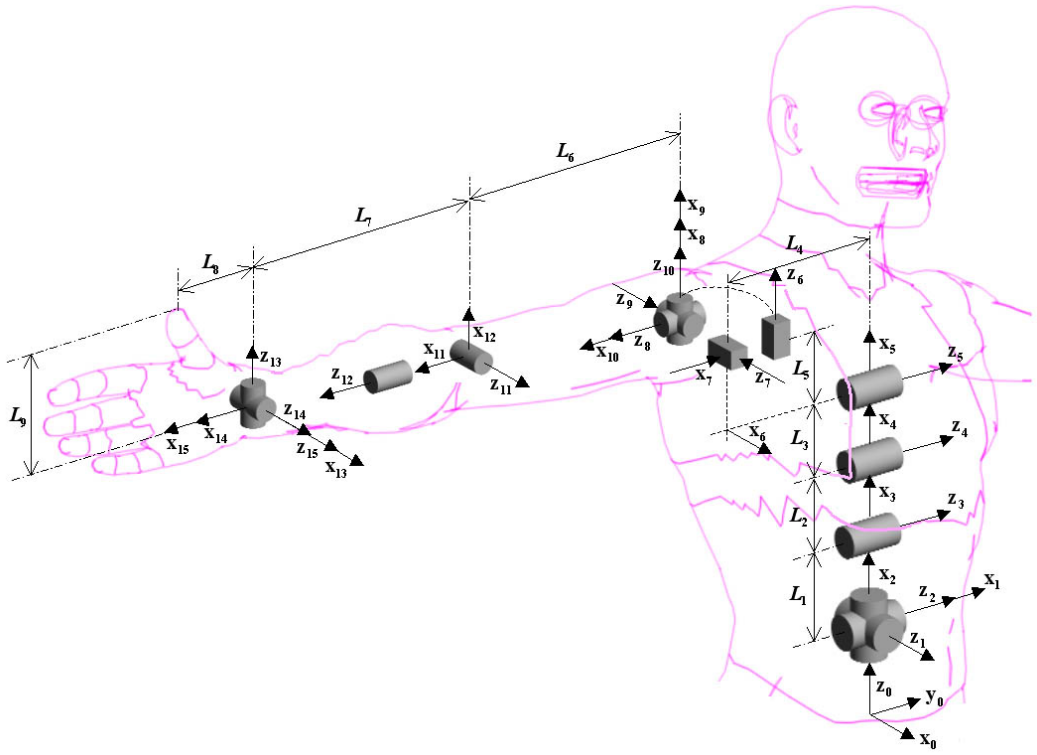

Figure 6 Modeling of the torso-shoulder-arm

The torso, shoulder and arm are modeled using 15 DOFs in total (Figure 6) as described above. The joint limits based on the experiments on three human subjects are $-\pi/6 \le q_1 \le \pi/6$, $-\pi/12 \le q_2 \le \pi/12$, $-\pi/18 \le q_3 \le \pi/6$, $-\pi/18 \le q_4 \le \pi/6$, $-\pi/18 \le q_5 \le \pi/6$, $-\pi/18 \le q_6 \le \pi/6$, $-3.81 \le q_7 \le 3.81$, $-3.81 \le q_8 \le 3.81$, $-\pi/2 \le q_9 \le \pi/2$, $-2\pi/3 \le q_{10} \le 11\pi/18$, $-\pi/3 \le q_{11} \le 2\pi/3$, $-5\pi/6 \le q_{12} \le 0$, $-\pi \le q_{13} \le 0$, $-\pi/3 \le q_{14} \le \pi/3$, $-\pi/9 \le q_{15} \le \pi/9$.

Formulation

In order to obtain a systematic representation of any serial kinematic chain, we define $\mathbf{q} = \begin{bmatrix} q_1 & \dots & q_n \end{bmatrix}^T \in \mathbf{R}^n$ as the vector of *n*-generalized coordinates defining the motion of

a limb with respect to another, where q_i is the individual DOF variable. The position vector function (shown in Figure 6) generated by a point of interest written as a multiplication of rotation matrices and position vectors is expressed by

$$\mathbf{x}(\mathbf{q}) = \begin{bmatrix} x(\mathbf{q}) \\ y(\mathbf{q}) \\ z(\mathbf{q}) \end{bmatrix} = \sum_{i=1}^{i=n} [\prod_{j=1}^{j=i-1} {}^{j-1}\mathbf{R}_j]^{i-1}\mathbf{p}_i = \mathbf{\Phi}(\mathbf{q}) \tag{1}$$

where both ${}^{i}\mathbf{p}_j$ and ${}^{i}\mathbf{R}_j$ are defined using the Denavit-Hartenberg (D-H) representation method (Denavit and Hartenberg 1955) such that

$${}^{i-1}\mathbf{R}_i = \begin{bmatrix} \cos q_i & -\cos\alpha_i \sin q_i & \sin\alpha_i \sin q_i \\ \sin q_i & \cos\alpha_i \cos q_i & -\sin\alpha_i \cos q_i \\ 0 & \sin\alpha_i & \cos\alpha_i \end{bmatrix}$$

$$\text{and } {}^{(i-1)}\mathbf{p}_i = \begin{bmatrix} a_i \cos q_i & a_i \sin q_i & d_i \end{bmatrix}^T \tag{2}$$

where q_i is the joint angle from $\mathbf{x}_{i-1}$ axis to the $\mathbf{x}_i$ axis, d_i is the shortest distance between $\mathbf{x}_{i-1}$ and $\mathbf{x}_i$ axes, a_i is the offset distance between $\mathbf{z}_i$ and $\mathbf{z}_{i-1}$ axes, and α_i is the offset angle from $\mathbf{z}_{i-1}$ and $\mathbf{z}_i$ axes.

Since the minimum jerk model to predict point-to-point motion trajectories is well accepted and experimentally verified (Flash and Hogan, 1985), We will first adopt the minimum jerk mathematical model to get a desired Cartesian path, and then convert it to joint coordinates with the objective to address the problem in joint space. Furthermore, because joint displacements as a function of time are non-uniform (free-form) curves, we will use the concept of B-spline curves (Pigel 1997) because of their many robust properties such as differentiability, local control and convex hull. We will then implement a numerical optimization algorithm to compute the control points

characterizing the B-spline curves, where we will utilize *Discomfort*, *Non Consistence*, *Non Smoothness* and *Non Continuity* as cost functions while using distances to the desired path at selected points as a set of constraints. The end result is an optimization-based method using human performance measures as an effective method for calculating joint path trajectories that look and feel most natural.

We will use B-splines to represent joint displacements as a function of time, one for each joint. In the following subsections, we will first introduce basic concepts of B-splines followed by expressions of joint B-spline functions used in our formulation. The B-spline curve of joint *j* can be obtained as

$$q_j(t) = \sum_{i=0}^{m} N_{i,3}(t) P_i^j \quad 0 \le t \le t_f, \; j = 1, 2, ..., n \tag{3}$$

where $N_{i,3}(t)$ is the base functions, P_i^j are control points for joint j and the total number of control points for joint j is $m+1$ (Pigel 1997).

The overall procedure is presented in Figure 7, and the path prediction module is refined and shown in Figure 8. The input to the algorithm are the start and end points of the motion, the position of the via point for a curved path in case of obstacle avoidance, DH parameters of the human model and the time desired to travel along the path. The absolute time is not very important here and it is the relative time at that instant that determines the shape of the velocity. The planning in Cartesian space is to find a 3-D path by minimizing jerk (Flash and Hogan, 1985). The path then is forwarded to the optimization module in joint space, which is to find a set of control points for the joint B-

splines that minimize discomfort and maximize the consistence, smoothness and continuity of joint movements with the hand moving along the path. This module actually does the transformation from Cartesian space to joint space.

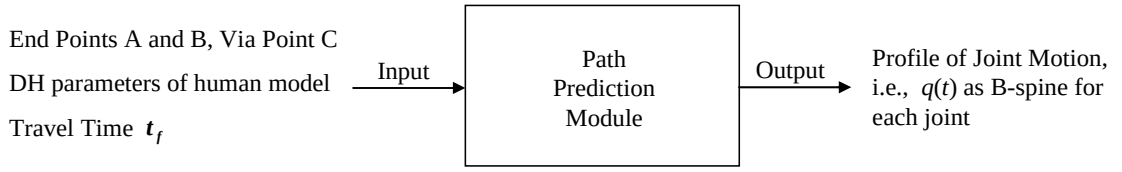

Figure 7 Path prediction illustration

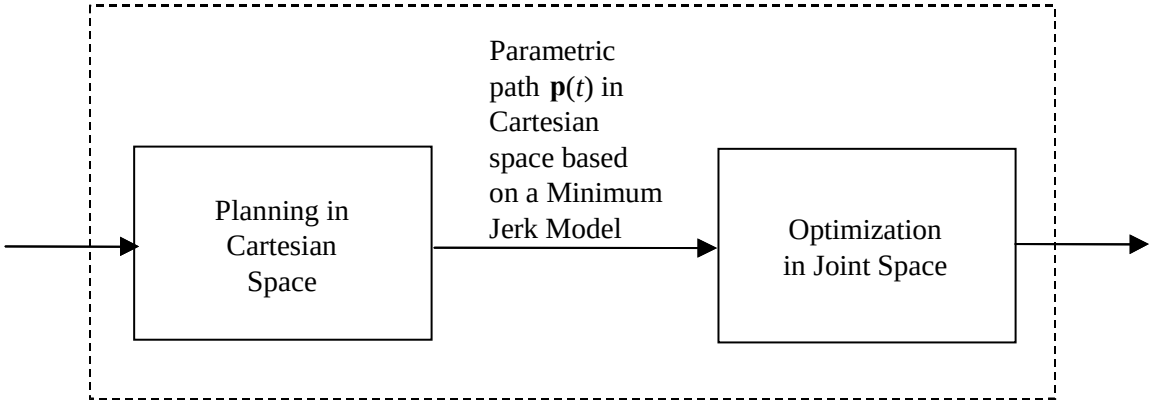

Figure 8 Refined path prediction module

When we have the start and end points, the posture prediction algorithm (Mi *et al*. 2002) is used first to predict the natural postures at the start and end points. That means one can obtain P_0^j and P_m^j, where $j = 1,...,n$. Therefore, the optimization problem is defined as

Find P_i^j, $i = 1,...,m-1$, $j = 1,...,n$

Minimize

$$\text{cost} = w_1 f_{discomf} + w_2 f_{inconsistency} + w_3 f_{nonsmoothness} + w_4 f_{noncontinuity} \tag{4}$$

Subject to

$$\| \mathbf{x}(\mathbf{q}(t)) - \mathbf{p}(t) \| = \| \mathbf{x}(\sum_{i=0}^{m} N_{i,3}(t)\mathbf{P}_i) - \mathbf{p}(t) \| < \varepsilon \tag{5}$$

$$q_j^L \le P_i^j \le q_j^U \tag{6}$$

where $0 \le t \le t_f$, ε is a small positive number as the tolerance; $\mathbf{P}_i = \begin{bmatrix} P_i^1 & \dots & P_i^n \end{bmatrix}^T$; $\mathbf{p}(t)$ is the path obtained from the planning in Cartesian space phase; w_1, w_2, w_3 and w_4 are the weights added to each performance index.

(1). The *discomfort function* of all joints:

$$f_{discomf}(\mathbf{q}) = \sum_{j=1}^{n} \xi_j \left(q_j - q_j^N \right)^2 = \sum_{j=1}^{n} \xi_j \left(\sum_{i=0}^{m} N_{i,3}(t) P_i^j - q_j^N \right)^2 \tag{7}$$

where q_j^N is the neutral position of a joint measured from the starting home configuration, ξ_j is a weight function assigned to each joint for the purpose of giving importance to joints that are typically more affected than others.

(2). *The inconsistency function*: By comparing the two postures (initial and end points), an overall changing trend of each joint (increasing or decreasing) can be predicted to avoid the abrupt change of the joint velocity. As a result, the consistency between the joint rate change (first derivative) and predicted overall trend is evaluated and will be added to the cost function. The detailed formulation of this consistency is as follows

$$\left.\begin{matrix}\mathbf{x}_0 \rightarrow \mathbf{q}^0 \\ \mathbf{x}_f \rightarrow \mathbf{q}^f\end{matrix}\right\} \rightarrow trend_i = \begin{cases} 1 & \text{if } (q_j^f - q_j^0) \geq 0 \\ -1 & \text{if } (q_j^f - q_j^0) < 0 \end{cases} \tag{8}$$

and

$$f_{inconsistency} = \sum_{j=1}^{n} (\left| sign(\dot{q}_j(t)) - trend_j \right| + 1) \left| \dot{q}_j(t) \right| \tag{9}$$

where

$$sign(\dot{q}_j(t)) = \begin{cases} 1 & \text{if } \dot{q}_j(t) \geq 0 \\ -1 & \text{if } \dot{q}_j(t) < 0 \end{cases} \tag{10}$$

The (+1) in Eq. (9) is to make the amplitude of the joint rate change still has an effect towards optimizing a smooth joint trajectory when the first term within the parenthesis is evaluated to be zero. The multiplication with the amplitude of this joint change rate is to enforce the underlying assumption that the smaller the joint angle change rate is, the smoother the joint trajectory will be. It also has significant effect on the optimization process, by not only qualifying the consistency, but also quantifying it so as to avoid the zero gradient of this objective, which is characteristic of an ill-stated optimization problem statement.

(3). *The non smoothness function*: The second derivative of the joint trajectory is considered in a non smoothness function as

$$f_{nonsmoothness} = \sum_{j=1}^{n} (\ddot{q}_j(t))^2 \tag{11}$$

(4). *The non continuity function*:

$$f_{noncontinuity} = \sum_{j=1}^{n} \left| \dot{q}_j^0 \right| + \sum_{j=1}^{n} \left| \dot{q}_j^f \right| \tag{12}$$

Once the control points of joint curves are selected by the iterative optimization algorithm, the cost function of Eq. (4) can be integrated (we integrate the first three terms and add the fourth term to it) to obtain the total cost at any point along the path. The same principle applies to the distance, where the total deviation along the path can be obtained by the integration of the distance between the calculated and desired paths from the start to the end points. In our algorithm, for simplicity, the cost function and distance constraints are evaluated by selecting representative points on the path where higher density is distributed close to the ends (total number of 43 have been selected). Since each joint's profile has $m+1$ control points, the total number of the design variables will be $n(m+1)$ initially. In our calculation, the joint values at the start and end have been obtained directly using the posture prediction algorithm, where we only need to calculate the remaining $m-1$ control points for each joint, i.e., the design variables for the optimization are reduced to $n(m-1)$.

Illustrative Examples

Based on simulation experiments, a set of weights (50, 100, 1, 1000) have been selected for w_1, w_2, w_3 and w_4 and modified feasible direction method has been used for the optimization. The overall calculation takes about 17 to 18 seconds on a 1.8GHz Pentium4 CPU with 512M RAM, which makes it possible to be used in real time on a higher speed end workstation with dual processors. An interface has been implemented in 3D Studio Max, which can interact with user, call the path prediction algorithm to do calculation, show results and animate human motions in real time.

(1). Point-to-point example:

Figures 9 to 13 are snapshots of a predicted motion, where the digital human starts from one point and goes to a target. The small spheres on the path are the constraints enforced on the hand position when predicting the joint B-splines. From the time stamps of the shown snapshots, it is easy to observe that hand moves more slowly at the start and end than in the middle. This is so-called bell shape velocity profile, a characteristic of a smooth and natural human arm movement (Flash and Hogan, 1985) and predictability of this profile is actually the strength of the minimum jerk model. The predicted joint profiles for the 15 joints are shown in Figure 14, from which we can see each joint moves smoothly towards the final position.

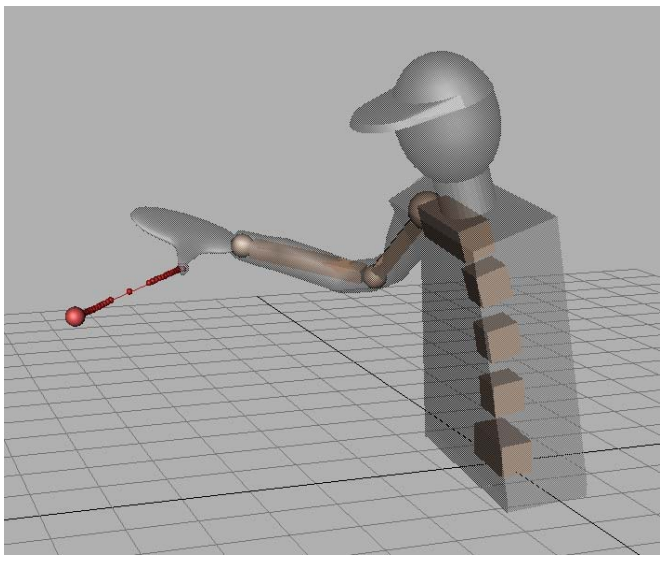

Figure 9 Predicted motion 1 at time 0

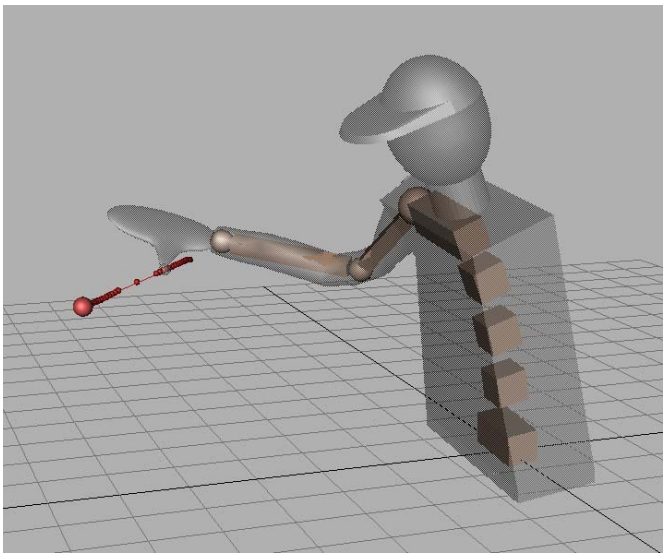

Figure 10 Predicted motion 1 at time $0.35t_f$

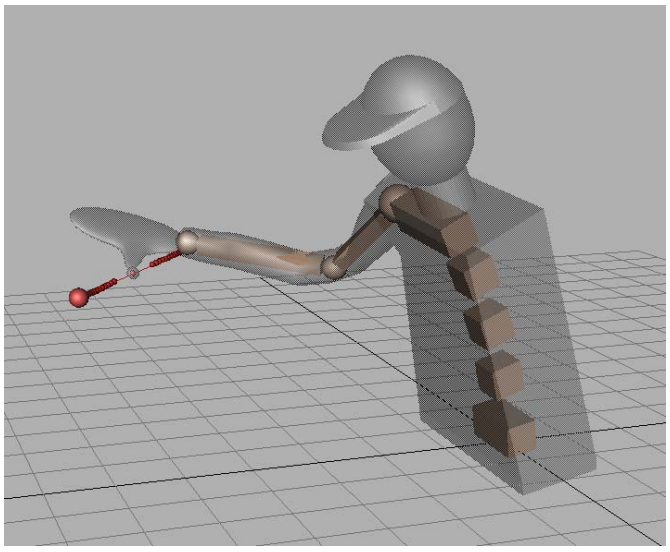

Figure 11 Predicted motion 1 at time $0.5t_f$

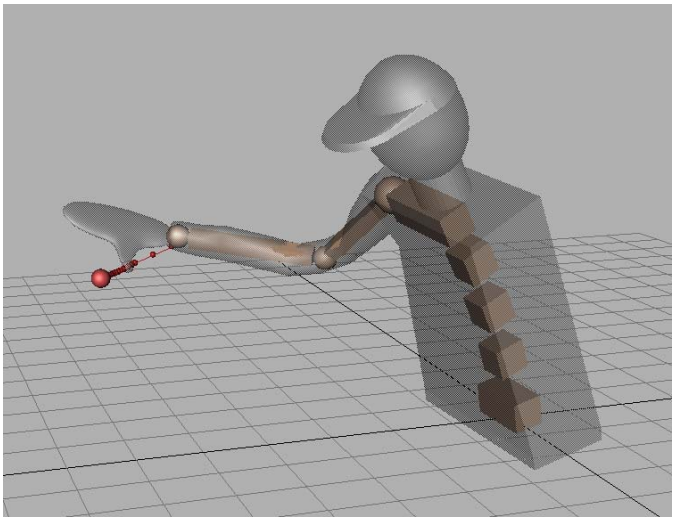

Figure 12 Predicted motion 1 at time $0.65t_f$

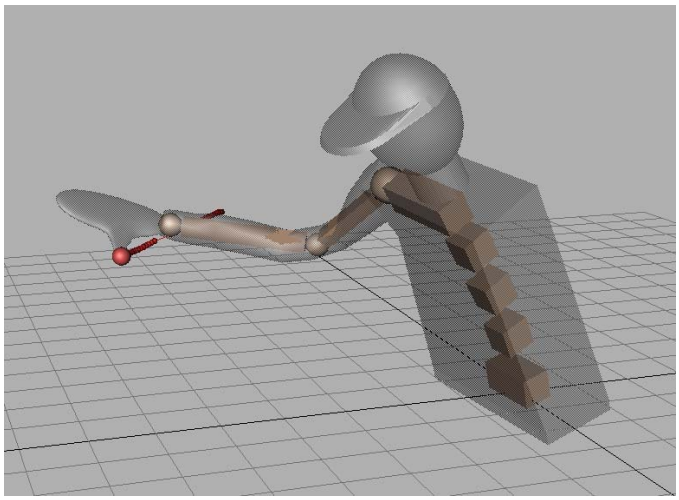

Figure 13 Predicted motion 1 at time t_f

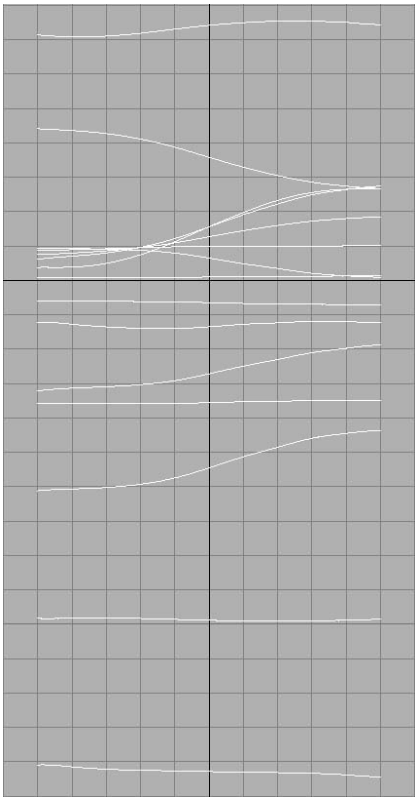

Figure 14 Predicted joint splines for motion 1

(2). ***Curved and obstacle avoidance example***

For curved and obstacle avoidance movements, it is assumed that the hand is required, in the motion between the end points, to pass through a third specified point (for example, an artificial intelligence engine can provide a via point to pass so as to go around the obstacle by examining the diameter of the obstacle). So given start and end points, and a third via point, a curved path in Cartesian space can be first generated (Flash and Hogan, 1985), while the time passing through the via point is first solved. Figures 15 to 19 give the snapshots of such movement while the digital human begins moving from an initial posture with all the joint angles at zero. The big green sphere is the via point and the curve is the Cartesian path predicted using minimum jerk model. The small spheres are where distance constraints are enforced during the optimization for joint splines. The

straight line is shown just for easy comparison with the curved path. The joint profiles shown in Figure 20 indicate the smooth movement of each joint.

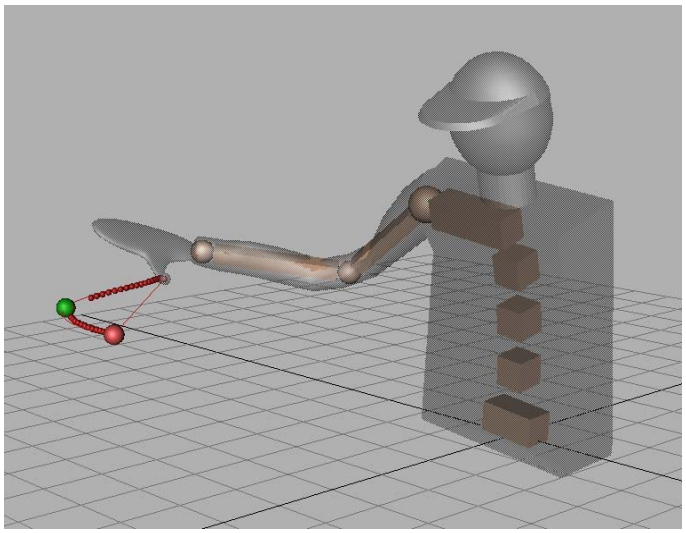

Figure 15 Predicted motion 2 with a via point at time 0

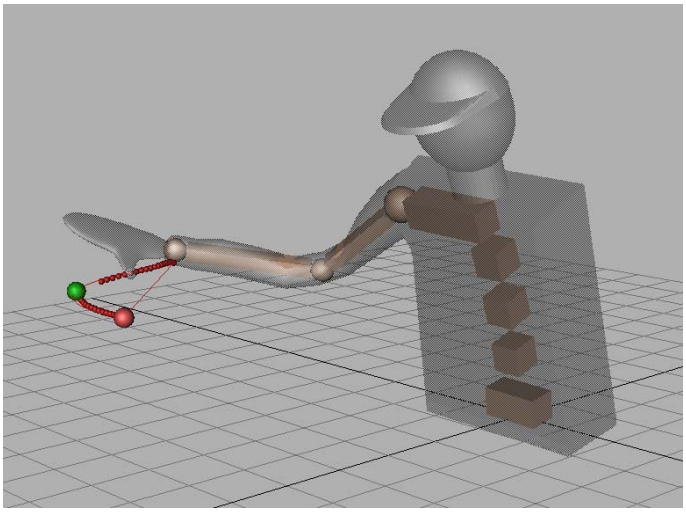

Figure 16 Predicted motion 2 with a via point at time $0.3t_f$

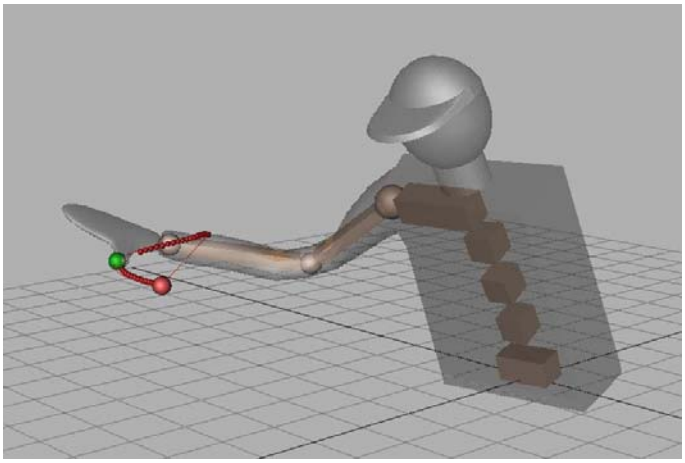

Figure 17 Predicted motion 2 with a via point at time $0.5t_f$

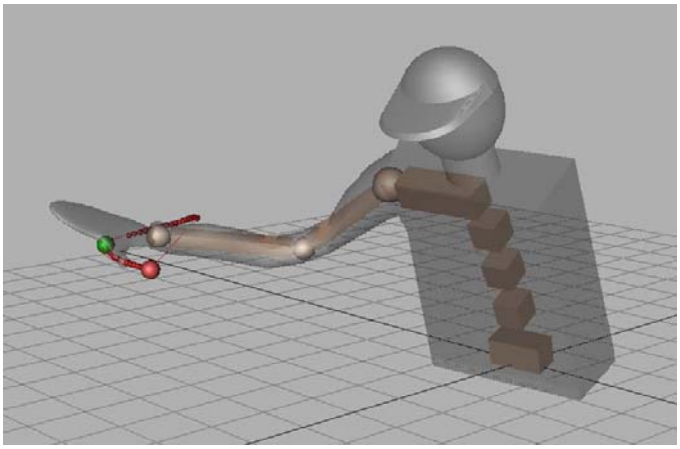

Figure 18 Predicted motion 2 with a via point at time $0.7t_f$

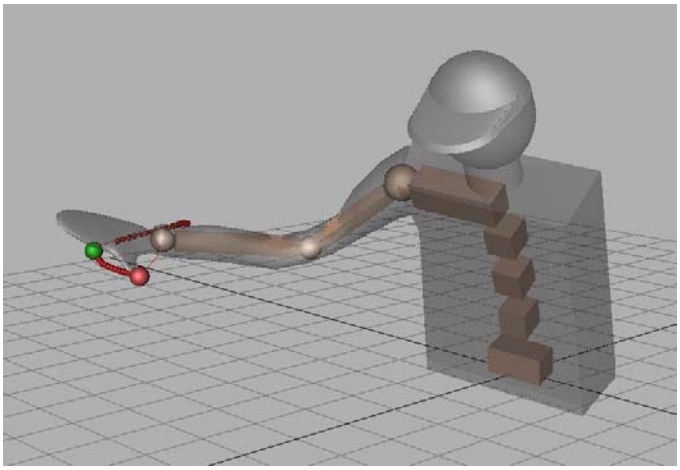

Figure 19 Predicted motion 2 with a via point at time t_f

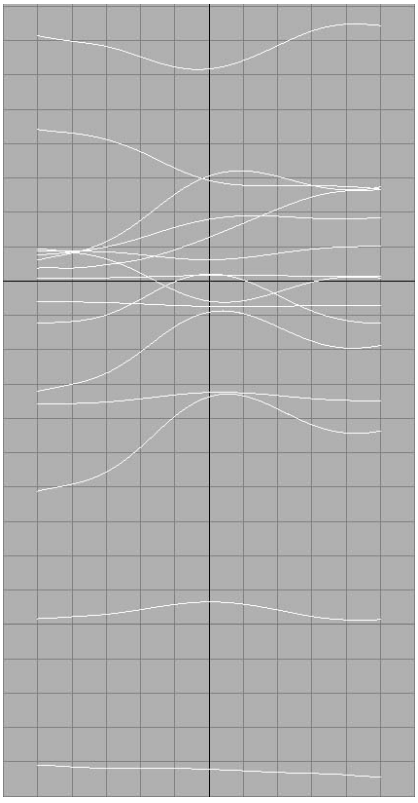

Figure 20 Predicted joint splines for motion 2 with a via point

As shown from the figures, the proposed method and algorithm can predict smooth and graceful movements of upper body even for a nonlinear (curved) path.

Conclusions

The proposed method for predicting joint profiles is general and is broadly applicable to any type of path, linear (straight) or nonlinear (curved) path trajectories. Nonlinear paths are applicable to obstacle avoidance problems, where trajectories are deviated from the typical linear point to point motion with minimum jerk. It was shown that a mathematical formulation applicable to any number of DOFs has been developed and demonstrated, were the joint profiles as a function of time are predicted. Each joint profile has been defined by a smooth B-spline, where control points are calculated using a novel optimization-based algorithm. It was shown that given any start or end points, or given a via point (a predefined intermediary point), our algorithm will first check and determine if these points fall within the reachable workspace of the digital human model. Once deemed within reach, a Cartesian path (including the time to traverse through the via point) is first predicted based on a minimum jerk cost function (within an iterative optimization algorithm), followed by the calculation of joint profiles characterized by B-splines, where the objective to minimize a discomfort function, non consistence function, non smoothness function, and non continuity function. It was also shown that the experimental code associated with this formulation was implemented in a graphical real-time simulation interface. The algorithm is shown to be robust and can be extended to a real time environment.

Acknowledgements

This research was funded by the US Army TACOM project: Digital Humans and Virtual Reality for Future Combat Systems (FCS).

Reference

1. Abdel-Malek, K., Yu, W., Tanbour, E. and Jaber, M., 2001, "Posture prediction versus inverse kinematics", *Proceedings of the ASME Design Automation Conference*, Pittsburgh, PA.
2. Alexander, R. M., 1997, "A minimum energy cost hypothesis for human arm trajectories," Biological Cybernetics, Vol. 76, pp. 97-105.
3. Barraquand, J. and Latombe, J.C., 1991, "Robot motion planning: a distributed representation approach", *International Journal of Robotics Research*, Vol. 10, No. 6.
4. Bobrow, J.E., 1988, "Optimal robot path planning using the minimum-time criterion," *IEEE Journal of Robotics and Automation*, Vol. 4, No. 4, pp. 443-450.
5. Brooks, R. A. and Lozano-Perez, T., 1983, "A Subdivision Algorithm in Configuration Space for Findpath with Rotation," *Proc. Eighth Int. Joint Conf. on Artificial Intelligence*, Karlsruhe, W. Germany, pp.799-806.
6. Constantinescu, D. and Croft, E.A., 2000, "Smooth and time-optimal trajectory planning for industrial manipulators along specified paths", *Journal of Robotics Systems*, Vol.17, No. 5, pp. 233-249.
7. Denavit, J. and Hartenberg, R.S., 1955, "A kinematic notation for lower-pair mechanisms based on matrices", *Journal of Applied Mechanics*, Vol. 77, pp. 215-221.
8. Flash, T. and Hogan, N., 1985, "The coordination of arm movements: an experimentally confirmed mathematical model", *The Journal of Neuroscience*, Vol. 5, No 7, pp.1688-1703.
9. Hogan, N. and Flash, T., 1987, "Moving gracefully: quantitative theories of motor coordination," *TINS*, Vol. 10, No. 4, pp. 170-174.
10. Kavraki, L.E., Svestka, P., Latombe, J.C. and Overmars, M., 1996, "Probabilistic roadmaps for path planning in high-dimensional configuration spaces", *IEEE Transactions on Robotics and Automation*, Vol. 12, No. 4, pp. 566-580.
11. Kawato, M., Isobe, M., Maeda, Y. and Suzuki, R., 1988, "Coordinates transformation and learning control for visually-guided voluntary movement with iteration: a Newtonlike method in a function space", *Biological Cybernetics*, Vol. 59, pp. 161-177.
12. Khatib, O., 1986, "Real-time obstacle avoidance for manipulators and mobile robots," *International Journal of Robotics Research*, Vol. 5, No. 1, pp. 90-98.
13. Khatib, O., Yokoi, K., Brock, O., Chang, K. and Casal, A., 1999, "Robot in human environments: basic autonomous capabilities", *The International Journal of Robotics Research*, Vol. 18, No. 7, pp. 684-696.
14. Lozano-Perez, T., Mason, M. T. and Taylor, R. H., 1984, "Automatic Synthesis of Fine-Motion Strategies for Robots," *International Journal of Robotics Research*, Vol. 3, No. 1, 1984, pp.3--24.
15. Li, H. and Ceglarek, D., 2002, "Optimal trajectory planning for material handling of compliant sheet metal parts," *Journal of Mechanical Design, Transactions of the ASME*, Vol. 124, n 2, pp. 213-222.

16. Mi, Z., Yang, J., Abdel-Malek, K., 2002, "Real-Time Inverse Kinematics for Humans," DETC2002/MECH-34239, *Proceedings of 2002 ASME Design Engineering Technical Conferences*, Montreal, Canada.
17. Nelson, W.L., 1983, "Physical principles for economies of skilled movements," *Biological Cybernetics*, Vol. 46, pp. 135-147.
18. Ohta, K., Svinin, M.M., Luo, Z.W., and Hosoe, S., 2003, "On the Trajectory Formation of the Human Arm Constrained by the External Environment," *Proceedings of the 2003 IEEE International Conference on Robotics & Automation*, pp.2884-2891.
19. Piegl, L., and Tiller, W., "The NURBS Book," Springer Verlag, 1997.
20. Plamondon, R., 1995, "A kinematic theory of rapid human movements: Part I. Movement representation and generation", *Biological Cybernetics*, Vol. 72, pp. 295-307.
21. Plamondon, R., 1995, "A kinematic theory of rapid human movements: Part II. Movement time and control", *Biological Cybernetics*, Vol. 72, pp. 309-320.
22. Plamondon, R., 1998, "A kinematic theory of rapid human movements: Part III. Kinetic outcomes", *Biological Cybernetics*, Vol. 78, pp. 133-145.
23. Pugazhenthi, S., Nagarajan, T., Singaperumal, M., 2002, "Optimal trajectory planning for a hexapod machine tool during contour machining," *Proceedings of the Institution of Mechanical Engineers, Part C: Journal of Mechanical Engineering Science*, Vol. 216, n 12, p 1247-1256.
24. Quinlan, S. and Khatib, O., 1993, "Elastic bands: Connecting path planning and control", *Proc. of the Int. Conf. on Robotics and Automation*, Vol. 2, pp. 802-807.
25. Saramago, S.F.P. and Steffen Jr, V., 2000, "Optimal Trajectory Planning of Robot Manipulators in the Presence of Moving Obstacles, " *Mechanism and Machine Theory* 35(8), 1079–1094.
26. Saramago, S.F.P. and Steffen Jr, V., 1998, "Optimization of the Trajectory Planning of Robot Manipulators taking into account the Dynamics of the System," *Mechanism and Machine Theory* 33(7), 883–894.
27. Saramago, S.F.P., Ceccarelli, M., 2002, "An optimum robot path planning with payload constraints," Robotica, Vol. 20, pp. 395-404.
28. Taylor, R.H., 1979, "Planning and execution of straight line manipulator trajectories", *IBM J. Res. Devel.*, Vol. 23, No. 4, pp. 424-436.
29. Uon, Y., Kawato, M. and Suzuki, R., 1989, "Formation and control of optimal trajectory in human multijoint arm movement", *Biological Cybernetics*, Vol. 61, pp. 89-101.
30. Wolpert, D.M., Ghahramani, Z. and Jordan, M.I., 1995, "Are arm trajectories planned in kinematic or dynamic coordinates? An adaptation study", *Experimental Brain Research*, Vol. 103, pp. 460-470.
31. Yang, J., Abdel-Malek, K., Nebel, K., and Tanbour, E., 2003, "The Reach Envelope of a 9 Degree of Freedom Model of the Upper Extremity," (submitted) *International Journal of Robotics and Automation.*
32. Yun, W.M. and Xi, Y.G., 1996, "Optimum motion planning in joint space for robots using genetic algorithms", *Robotics and Autonomous Systems*, Vol. 18, pp. 373-393.